Title	Polarization-based fiber-optic delay lines
Authors	Riza, Nabeel A.
Publication date	1995-10-01
Original Citation	Riza, N. A. (1995) 'Polarization-based Fiber-optic Delay Lines', Proceedings of SPIE, 2560, Optical Technology for Microwave Applications VII; SPIE's 1995 International Symposium on Optical Science, Engineering, and Instrumentation, San Diego, CA, USA, pp. 120-129. doi: 10.1117/12.218516
Type of publication	Conference item
Link to publisher's version	10.1117/12.218516
Rights	© 2007 Society of Photo-Optical Instrumentation Engineers (SPIE). One print or electronic copy may be made for personal use only. Systematic reproduction and distribution, duplication of any material in this paper for a fee or for commercial purposes, or modification of the content of the paper are prohibited.
Download date	2024-03-02 17:58:41
Item downloaded from	https://hdl.handle.net/10468/10235

Polarization-based fiber optic delay lines

Riza, Nabeel

Nabeel A. Riza, "Polarization-based fiber optic delay lines," Proc. SPIE 2560, Optical Technology for Microwave Applications VII, (1 October 1995); doi: 10.1117/12.218516

Event: SPIE's 1995 International Symposium on Optical Science, Engineering, and Instrumentation, 1995, San Diego, CA, United States

Polarization-based Fiber-optic Delay Lines

Nabeel A. Riza
Center for Research & Education in Optics and Lasers (CREOL)
and the Department of Electrical & Computer Engineering
University of Central Florida
12424 Research Parkway, Suite 400, Orlando, FL 32826

Abstract

Multi-channel fiber-optic delay line architectures using optical polarization switching are proposed that use non-polarization maintaining single-mode fibers while still maintaining high extinction polarization properties of the switched optical beams. Critical birefringence compensation and noise reduction techniques are introduced and demonstrated for these delay lines showing high optical polarization extinction (> 39 dB) and electrical signal-to-noise ratio (> 92 dB) results.

2. Introduction

Recently, we introduced potentially low interconnection complexity, low insertion loss, three dimensional optical time delay units for transmit/receive mode phased array antenna applications [1]. These units use two dimensional spatial light modulators (SLMs) as optical polarization switching elements to form highly parallel, multichannel, switched optical delay lines using free-space or solid optics propagation delay. Preliminary results using nematic liquid crystal optical switching elements have indicated high on/off isolation within a time delay channel. A 1 X 2 nematic liquid crystal switch structure with > 35 dB optical isolation has been demonstrated. In addition, a single channel > 30 dB optical isolation nematic liquid crystal 1-bit, 3.33 ns optical time delay unit has been demonstrated. More recently, a 25 channel optical time delay unit has also been characterized showing low -42 dB electrical crosstalk values.

Certain applications require long time delays that are impractical to achieve using free-space or solid optics. Such applications include radar simulation and testing, rf transversal filtering and multi-path cancellation, and true-time delay control for large (e.g., 5 meter diameter) or distributed/conformal phased array antennas.

This paper describes novel N-bit switched fiber-optic delay line structures using polarization-based optical switching via two dimensional polarization-mode SLMs such as nematic liquid crystal SLMs, ferroelectric liquid crystal (FLC) SLMs, magneto-optic SLMs, or multiple quantum well SLMs. Here, unlike the free-space delay medium used in the previously demonstrated delay lines [2-3], optical fibers are used for providing longer duration (> 5 ns) time delays. The optical structure is designed such that unwanted polarization effects are minimized so that high extinction ratio polarization optical switching can be maintained. This is achieved without using costly polarization maintaining (PM) single mode fibers. In fact, the fiber delay line is insensitive to the slowly changing fiber birefringence effects due to external conditions such as temperature variations and mechanical stresses. This paper describes the fundamental concepts for this polarization tolerance and its use in an N-bit switched fiber-optic delay line with proof-of-principle experimental results. In addition, we demonstrate a novel noise reduction technique proposed in [2] that is vital for high performance polarization-switching based delay lines.

3. Principles of the Novel Switched Fiber Optic Delay Line using Birefringence Compensation

The use of a passive technique for compensation of polarization changes induced by any optical medium birefringence on a propagating light beam was proposed in [4], where an optical beam retracing geometry coupled with a Faraday rotator/mirror set-up was used to eliminate the effects of the changing material birefringence on the input and output state of polarization (SOP). Later, this technique was used to suppress birefringence effects in optical fiber sensors [5]. In fact. today, many fiber-optic isolators use a similar mechanism to prevent unwanted feedback in many optical systems. In this paper, we show how the birefringence technique in [4] can be incorporated to form high performance non-PM fiber based switched multi-channel optical delay lines.

It is clear that systems based on polarization cannot tolerate changes in the desired state of polarization as it leads to unwanted effects such as signal fading, loss in optical heterodyning efficiency in interferometric systems, increase in unwanted noise sources, and overall higher loss in the system. Systems that use fibers must use PM fibers to retain the high degree of the desired SOP. Nevertheless, any changes in the PM fiber's optical birefringence caused by the changing environment or

0-8194-1919-2/95/$6.00

even the change in the optical wavelength can degrade the desired SOP of the travelling light beam. Moreover, PM fibers cost a lot more than regular telecom grade single mode fibers. Thus, particularly for our multi-channel delay line application, we need many fiber segments with a cascading architecture, and therefore we cannot tolerate any major changes in SOP caused by the fiber segments, or for that matter, any other component.

Fig.1 shows the top view of the proposed fiber birefringence compensated N-bit M channel switched fiber delay line where for example N=3 bits and M= 16 channels. Here 16 linearly polarized and collimated beams enter the system and pass through a 4 X 4 pixelated array of a polarization-mode SLM such as an FLC SLM. Each SLM pixel when turned-on has the capability to rotate the input beam linear polarization by 90 degrees. In the off-state, the pixel does not rotate the input beam polarization. The SLM combined with the PBS form a multichannel optical switch where depending on the SLM setting, beams are directed toward the fiber paths or straight through to the next SLM. For the case of an input horizontally polarized beam with the SLM pixel on, the SLM exited vertically polarized beam is deflected 90 degrees by the PBS into a fiber coupling lens (e.g., GRIN lens fiber collimator) that is connected to a single mode non-PM fiber of a certain desired length. The vertically polarized light input into the fiber exits the fiber via another fiber lens. At this stage, depending on the fiber birefringence the travelling light has suffered (this depends on the individual fiber and the external conditions), the fiber exit light is no longer vertically polarized and the SOP lies some where different on the Poincare sphere. This perturbed light passes through a Faraday rotator to strike a mirror that reflects the light back through the Faraday rotator and the birefringent fiber. It turns out that this beam retracing operation coupled with the Faraday rotator and mirror induce symmetry properties on the Poincare sphere rotations, causing the fiber entrance and exit polarization states to be always orthogonal points on the Poincare sphere. Thus, if vertically polarized light enters the non-PM fiber, then horizontally polarized light exits the fiber regardless of the birefringence effects in the fiber and the fiber-coupling optics. This preservation of the linear SOP is critical for operation of the proposed switched delay line. Note that the horizontally polarized light exiting the fiber after the mirror reflection travels through the PBS to be retraced through a quarterwave plate-mirror arrangement. The light returning from this mirror is again vertically polarized and is reflected by 90 degrees by the PBS to enter the next SLM that forms the next bit in the delay line.

Fig.2 shows the detailed movement of the SOP on the Poincare sphere and its equatorial projection for the case when the entrance polarization is horizontal (point H) [4]. In this case, the presence of birefringence translates point H to point B by means of a rotation around the axis 2θ by an angle Δ. Half of the Faraday rotator operation appears on the north hemisphere (path BM). The mirror reflects the point M to M' and the Faraday rotator acts on the south hemisphere (path M'B'). This point B' is symmetric to point B and by means of a further rotation around the axis 2θ, the new point is V, i.e., the vertical SOP.

4. Features and System Issues

It is clear from Fig.1 that the proposed switched fiber optic delay line has certain key features. The use of fibers for the delay medium using the SOP compensated design results in a compact assembly as (a) half the length of the fibers is required because of the reflective geometry in the delay path, (b) only one large area Faraday rotator-mirror assembly and one large area quarterwave plate-mirror assembly are required because of the flexibility of the fibers to bunch together in the interconnection process, (c) the fibers can be coiled and stressed/packaged in any ultra-compact way because they do not effect the SOP of the processed beams, and (d) the use of a few bulk optical elements and 2-D SLMs. Furthermore, this design allows the use of both horizontal and vertical stacking to increase the channel count.

Nevertheless, the system does have its design constraints. Because we are using fiber collimating lenses, there is a certain beam divergence angle associated with these devices that determines the maximum fiber-to-fiber working distance. Typical values are 1-3 milliradian single mode beam divergence with a 1.0 mm diameter single mode beam, with a typical maximum fiber-to-fiber efficient coupling distances of 10 cm. Thus, without the use of imaging lenses, the working distance is limited which in turn implies a design trade off in the number of bits and the number of system channels. A typical design would be a 5 X 5 channel 6-bit design using 10 mm side cube PBSs, with the maximum package length being about 6.5 cm. Because stacking is possible, the channel count can be increased relatively easily by adding another set of components. Note that the SLMs, Faraday rotator-mirror, and quarterwave plate-mirror assembly can be designed to accomodate later upgrading in channels and/or bits.

Another important issue is optical loss within the system. Because we are using fiber coupling lenses that typical have a loss of 0.5 dB when coupling light into or out of the fiber assembly, the number of bits in this system are limited because of the cascading nature of the delay line. Thus, where possible (i.e., for the shorter least significant bits of the delay line) use free-space or solid optics for the delay medium. This brings us to the next point as we observe Fig.1; namely, that the system in Fig.1 can also be used for a free-space/solid optics delay system. This system is shown in Fig.3. Optical delays can be achieved in free-space or a solid optics medium with a particular chosen refractive index for making compact delays. In addition, for the longer delays imaging optics can be used as shown in Fig.3. Here, because of the reflective geometry, a single imaging lens with half the imaging distance (compared to a two lens transmissive path) is required for the time delay, thus saving components and space compared to a transmissive system. Note that in this reflective delay line design, the delayed beam travels the PBS side/width three times while the straight/no-delay beam travels the PBS width once. Thus, the systems in Figures 1 & 3 have a built in-delay because of the reflective geometry; thus shorter external delay paths (fiber or free-space) need to be added. Thus, with reference to Fig.3, for most microwave and millimeter wave applications, clever non-fiber designs can be used with these delay lines. Nevertheless, for some critical applications, fiber delay is the only option for achieving the very long time delays. In this case, the proposed SOP compensated fiber-optic delay line design shown in Fig.1 must be preferred over other free-space/solid optics designs.

5. Switched Fiber Optic Delay Line using Noise Reduction

Fig.4 shows the simple noise reduction technique implemented in a birefringence compensated fiber optic delay line. Note that each delay bit structure at its output port needs an additional polarization switching SLM and a high extinction polarizer. This additional SLM sets the vertical and/or horizontal polarization output beams from the delay unit to one polarization that is aligned with the high extinction output polarizer/PBS. In this way, the unwanted noise signals can be rejected from the system. Because these delay lines are based on cascaded designs, it is all the more important to reset the beam quality before entering the next bit in the system. As was shown earlier, when using a cube PBS for the delay structure, a high extinction ratio polarizer has to be inserted at the deflected output port of the PBS to maintain high performance [1]. Note that this cannot be done in the reflective design shown in Fig.1 and 3 as this would block the light returning from the mirror. Thus, the noise reduction technique shown in Fig.4 is all the more critical in these reflective-mode designs using both fiber and/or free-space/solid-optics.

6. Noise Reduction and Birefringence Compensation Experiment

The noise reduction experimental setup for a 1-bit time delay structure is depicted in Fig.5. Two Thompson-polarizing beamsplitters (TBSs) are used to form a crossed polarization setup. The first one lets vertical or s-polarization to pass through and the second one lets horizontal or p-polarization to pass through it. Since the system needs to maintain the high state of polarization, optical components with high extinction ratio (ER) must be used. The ER is defined in dB as 10 log(max/min), where max/min is the ratio of the maximum output power in one polarization versus the minimum output power corresponding to the other orthogonal polarization. The ER for the crossed TBS setup was measured at 50.94 dB, while the NLC devices had optical on/off ratios of 34.52 dB, 38.09 dB and 35.44 dB. s-polarized light from a 13mW He-Ne laser passes through the first Thompson beamsplitter (TBS1). A NLC device (LC1) is inserted with its NLC director at 45° to the incident s-polarization. This NLC cell is a parallel-rub birefringent mode device, and is driven by a 0-5V, 1KHz square wave signal from a Wavetek Model 75 waveform generator. The NLC cell acts as a switch changing the polarization from s to p when it is in the "on" state, or lets the same polarization through when it is in the "off" state. The cube PBS acts as a path selector, directing light depending on the polarization of the incident beam. There are two paths in the system; the straight path and the delay path. In the straight path case, p-polarized light coming out of LC1 (LC1: "on") hits the PBS and travels straight through to the NLC device (LC2). LC2 is similar to LC1 and has its director at 45° to the incident p-polarization. LC2 is set in the "off" state such that it does not change the polarization of the incident beam, which then passes through the second Thompson beamsplitter (TBS2). On the otherhand, when LC1 is in the "off" state, the light stays s-polarized, and is deflected from the PBS towards a third NLC device (LC3) which is set to act as a quarter-wave plate having its axis at 45° with the incident s-polarization. When s-polarized light hits LC3, it changes to circular polarization. After reflection from the mirror (M1), this light passes through LC3 again, changing to p-polarization. The light passes through the PBS and hits a quarter-wave plate, having its axis at 45° with the incident p-polarization. After reflection from the mirror (M2), the beam is redirected through the quarter-wave plate and becomes s-polarized. This s-polarized light is deflected from the PBS towards LC2 which is set in the "on" state. s-polarization changes to p-polarization and passes through TBS2. The optical power measurements were made with a Newport Digital Power Meter model 815.

As Table 1 shows, good results were obtained for the electrical signal to noise ratio (SNR) and the optical polarization ER for the system using the noise reduction technique. The electrical SNR in dB is defined as 20log(signal optical power/noise optical power), where signal optical power is the power in the optical beam of the desired polarization that travels through the set delay or no-delay path of the time delay unit; all other optical power measured at the output is regarded as the noise optical power. The electrical SNR is important as the current (or voltage) generated by an optical detector at the output of the delay line is proportional to the incident light intensity, and this output eventually drives a signal processing component such as an antenna element in a radar or communication antenna array system. The key result from Table 1 is that for the case where no LC2 and TBS2 are present, i.e., no noise removal/suppression is used, the system performance deteriorates drastically. This is particularly severe as the cube PBS optical on/off performance is poor at its deflected port, and so some optical ER improvement technique must be used in the system. Our method does the job. As mentioned earlier, fibers change birefringence and hence optical polarization properties of a traveling optical beam that leads to noise generation in a polarization-based delay line system. Fig.6 shows the fiber birefringence compensation experimental setup for a 1-bit delay line. A Faraday rotator with a rotation power of 45° at 633 nm is inserted in the delay path. Instead of using a fiber with externally induced stress, the experiment is performed using a parallel-rub birefringent mode NLC device LC3 which had an electrically controllable birefringence. LC1 is set in the "off" state and LC2 in the "on" state. LC3 has its nematic director at 45° with the incident s-polarization. A 0 to π total (round trip) birefringence corresponds to a voltage change from 3.11V to 5.77 V. A series of measurements of the signal and noise powers were taken, as well as the p and s polarization powers for the output beam. Electrical SNR and optical ER measurements were obtained as a function of the total induced birefringence, and are shown in Fig.7. The measurements were obtained at 0.10 V steps of the peak driving voltage for LC3. The average value of the electrical SNR was $\overline{SNR} = 98.35\text{dB}$, while the average electrical SNR variation was $\overline{\Delta(SNR)} = \pm 0.584\text{dB}$. The average optical ER was $\overline{ER} = 39.20\text{dB}$ and the average optical ER variation was $\overline{\Delta(ER)} = \pm 0.0481\text{dB}$. These results indeed show that the fiber birefringence compensation technique using a reflection geometry with a Faraday rotator negate the unwanted polarization effects of a variable birefringent delay medium such as an optical fiber.

7. Fiber Birefringence Compensation Experiment using a Non-PM Single Mode Fiber

The birefringence compensation technique was also tested using a non-PM single mode fiber. The LC3 of the previous experiment was replaced by a 633 nm single mode fiber of length 1.76 m. A GRIN collimator-lens is attached to one end of the fiber, and the other end is cleaved. The light coming from the PBS was coupled into the fiber using an objective lens (×40, NA:0.65, FL=4.3 mm). The power input to the fiber was measured at 9.73 mW, while the power output was 5.80 mW, giving a total fiber assembly attenuation of -2.2 dB. This attenuation is due to the limited coupling efficiency of the objective-fiber system. The measured optical power between M1 and the Faraday rotator was 5.28 mW, and the power before the QWP was 1.98 mW. Considering the attenuation of the GRIN lens-fiber system (-2.2 dB), the expected value of the optical power before the QWP is 3.18 mW. This can be explained by the non-perfect coupling in the GRIN lens, mainly because the beam is not highly collimated. The output power of the TDU was 1.34 mW with a small variation of ±0.04 mW, and the noise power was 0.150 µW. That gives an electrical SNR of 79 dB. Note that if the coupling efficiencies for both ends of the fiber were higher, the signal would be stronger and thus the SNR would also be higher. The ER of the output beam was measured at 43.58 dB.

When stress is applied on the fiber, the output power is essentially not affected. It remains at the same level with the same variation of ±0.04 mW. Different kinds of stresses and temperature changes were tested, such as squeezing the fiber with fingers, pressing the fiber against the optical table with hand or metallic plate, holding the fiber with hands that had been warmed by rubbing, or just placing the fiber on the cold surface of the optical table. In order to show the importance of the Faraday rotator in the system, the rotator was replaced by a NLC device, that acts as a QWP, with its NLC director at 45° with the incident s-polarization. We immediately noticed that the QWP-mirror configuration cannot compensate for the fiber birefringence noise, and the system performance deteriorates drastically. Several stresses and temperature conditions were tested for this case as before. The output power of the TDU drastically changed depending on the external conditions. The electrical SNR drops significantly and varies from 40 dB to 59 dB depending on the induced fiber birefringence.

8. Novel Optical Delay Line Architectures based on Beam Displacing Prims

Previously, we have shown and demonstrated how cube PBSs [1] and Thompson-prism PBSs [2] can be used to make switched optical delay lines. Figures 8 to 10 show how polarizing beam displacing prisms (BDPs) can be used to form switched optical delay lines, including the efficient binary fiber-optic delay line structure. BDPs are high extinction polarization devices that can benefit certain optical delay line designs and will be demonstrated in future work.

9. Conclusion

In conclusion, a polarization-based noise reduction technique for optical delay lines has been proposed and demonstrated using a setup based on NLC optical switching devices, a cube PBS, and high quality Thompson PBSs. High electrical SNR (>92 dB) and optical ER (>50 dB) were obtained with this noise suppression method. Using a similar setup, with the addition of a Faraday rotator, a novel fiber birefringence compensation technique for switched optical delay lines was demonstrated for a 1-bit optical delay structure. High optical ER and electrical SNR were demonstrated (>39 dB and 98 dB, respectively), with low average variations (<0.1 dB and 1 dB, respectively) over the 0-π induced birefringence range. Other novel free-space, fiber, and solid-optics optical delay line structures have been introduced, including architectures based on polarizing beam displacing prisms. Future work relates to the experimental demonstration of these systems.

10. Acknowledgement

The author would like to thank N. Madamopoulos for the help in data acquisition for the experiments. Partial support for this work is provided by Office of Naval Research Grant No.N000149510988 through Dr. W. Miceli.

11. References

[1] N. A. Riza, ``Liquid crystal-based optical time delay units for phased array antennas,'' *IEEE/OSA Journal of Lightwave Tech*, Vol. 12, No.8, pp.1440-1447, August, 1994.
[2] N. A. Riza, ``Liquid crystal-based optical controllers for phased array antennas,''*SPIE Proc.*, Vol. 2155, pp.168-180, Los Angeles, California, Jan., 1994.
[3] D. Dolfi, P. Joffre, J. Antoine, J. P. Huignard, J. Roger, and P. Granger, ``Two dimensional optical beamforming networks,'' *SPIE Proc.*, Vol. 2155, pp.205-217, Los Angeles, California, Jan., 1994.
[4] M. Martinelli, `` A universal compensator for polarization changes induced by birefringence on a retracing beam,'' Optics Communications, Vol.72, No.6, pp.341-344, Aug., 1989.
[5] N. C. Pistoni and M. Martinelli, `` Birefringence effects suppression in optical fiber sensor circuits,'' International Conference on Optical Fiber Sensors, Paper 59, pp.125-128, Sydney, Australia 1990.

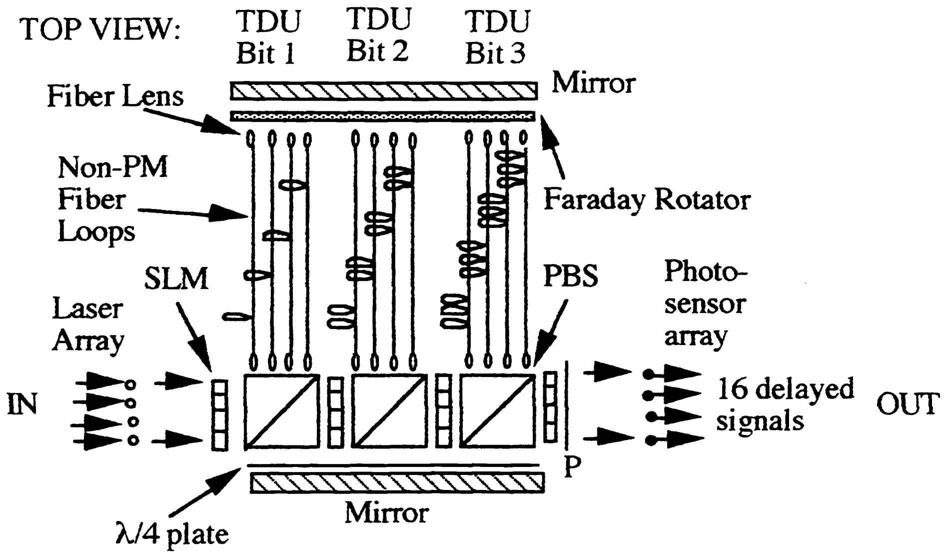

Fig.1 shows the top view of the proposed fiber birefringence compensated N-bit M channel switched fiber delay line.

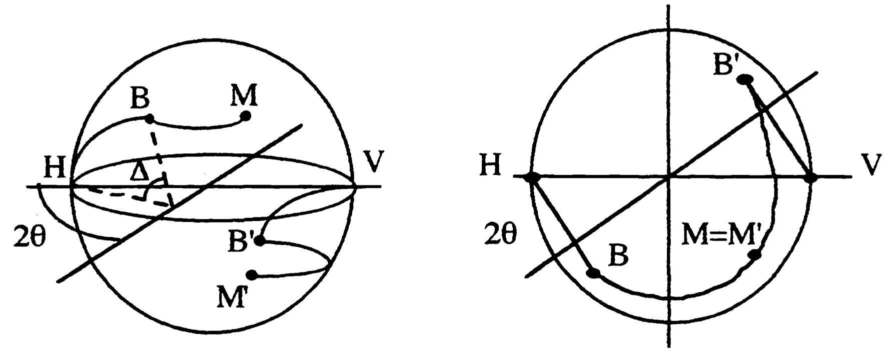

Fig.2 shows the detailed movement of the SOP on the Poincare sphere and its equatorial projection for the case when the entrance polarization is horizontal (point H).

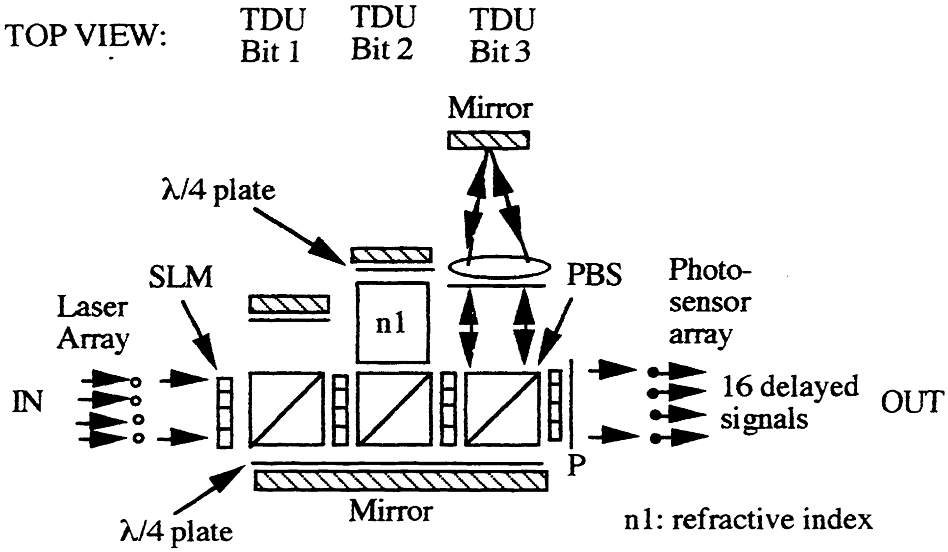

Fig.3 shows a free-space/solid optics delay system based on the delay line in Fig.3.

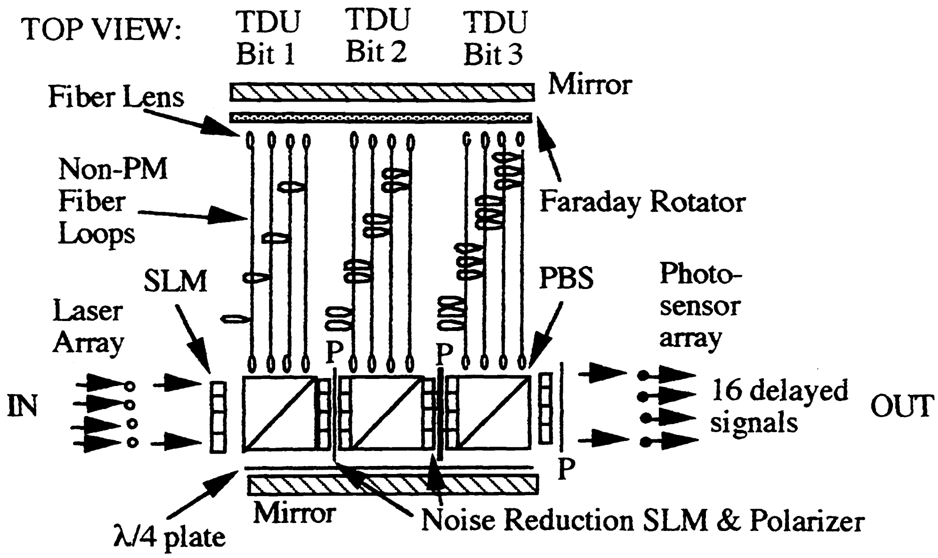

Fig.4 shows the top view of the proposed fiber birefringence compensated N-bit M channel switched fiber delay line using the novel noise reduction technique.

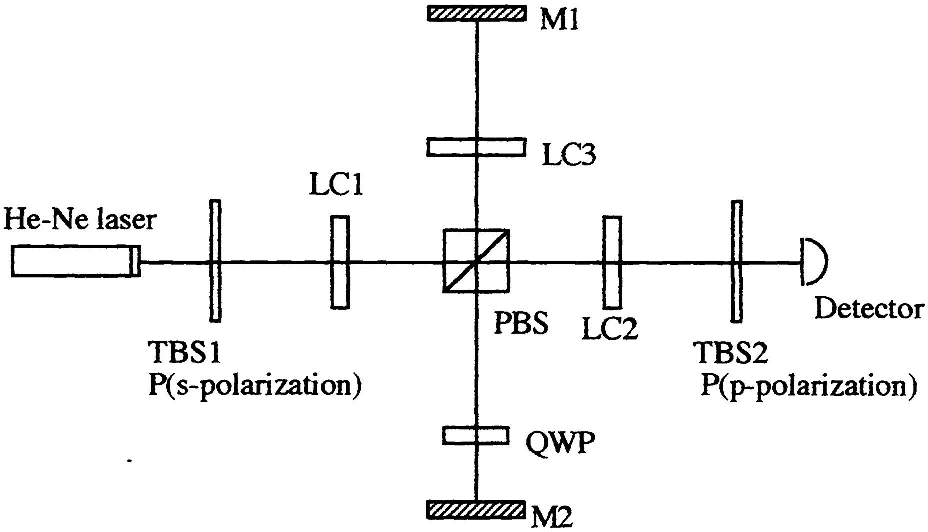

Fig.5 The experimental setup for the optical delay line noise reduction scheme. The NLC devices are driven by 0-5V, 1KHz square wave signal. The "on" or "off" operation can be selected by setting the V_p drive level.

	Straight Path	**Delay Path**
Electrical S/N (dB)	96.90	92.40
Electrical S/N (dB) (without noise reduction scheme)	49.40	28.88
Extinction ratio (dB)	50.75	50.43
Extinction Ratio (dB) (without noise reduction scheme)	24.22	14.77

Table 1: Electrical signal-to-noise ratio and optical extinction ratio measurements in dB for the delay-path and the straight-path of the optical delay line with and without the noise reduction scheme.

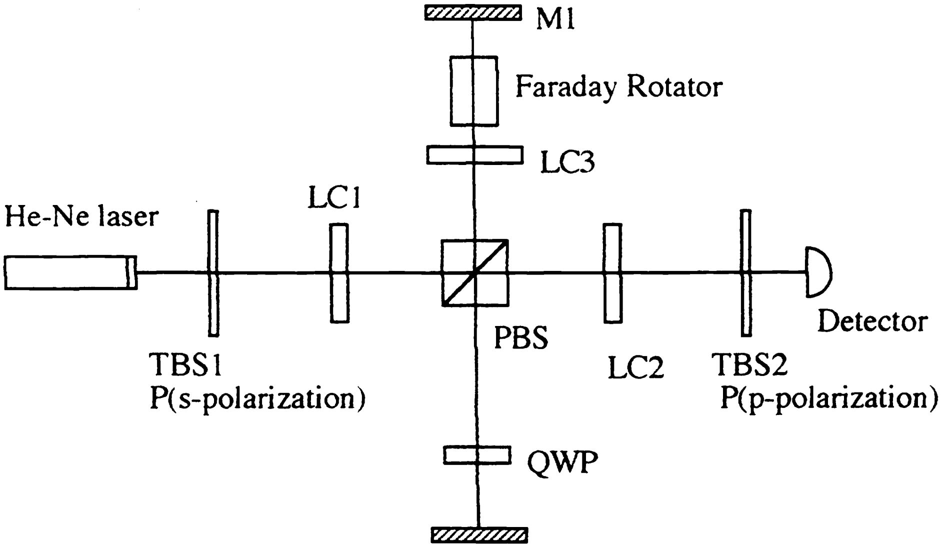

Fig.6 The experimental setup for the optical fiber birefringence compensation technique for the optical delay line. LC3 simulates a fiber with a variable birefringence by controlling the driving voltage of the NLC device.

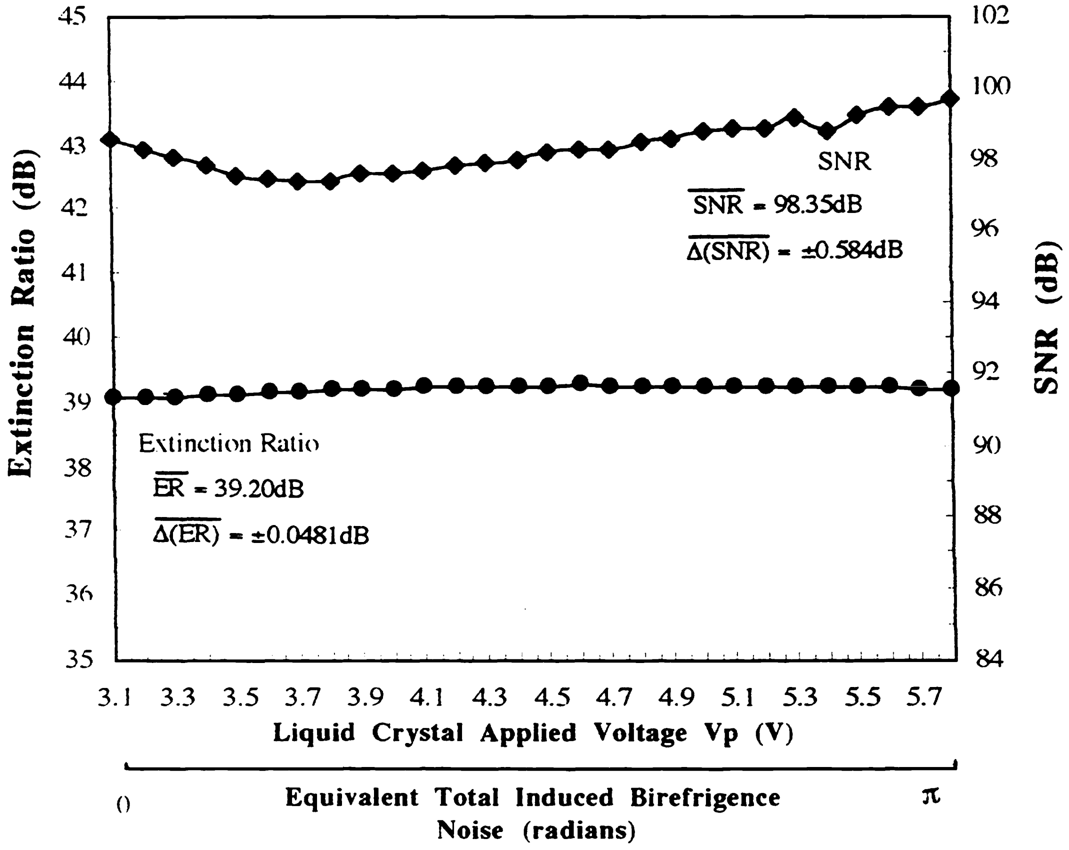

Fig.7 shows the optical extinction ratio and electrical signal-to-noise ratio measurements vs. the LC3 applied voltage and the equivalent total induced birefringence noise for the experiment in Fig.6.

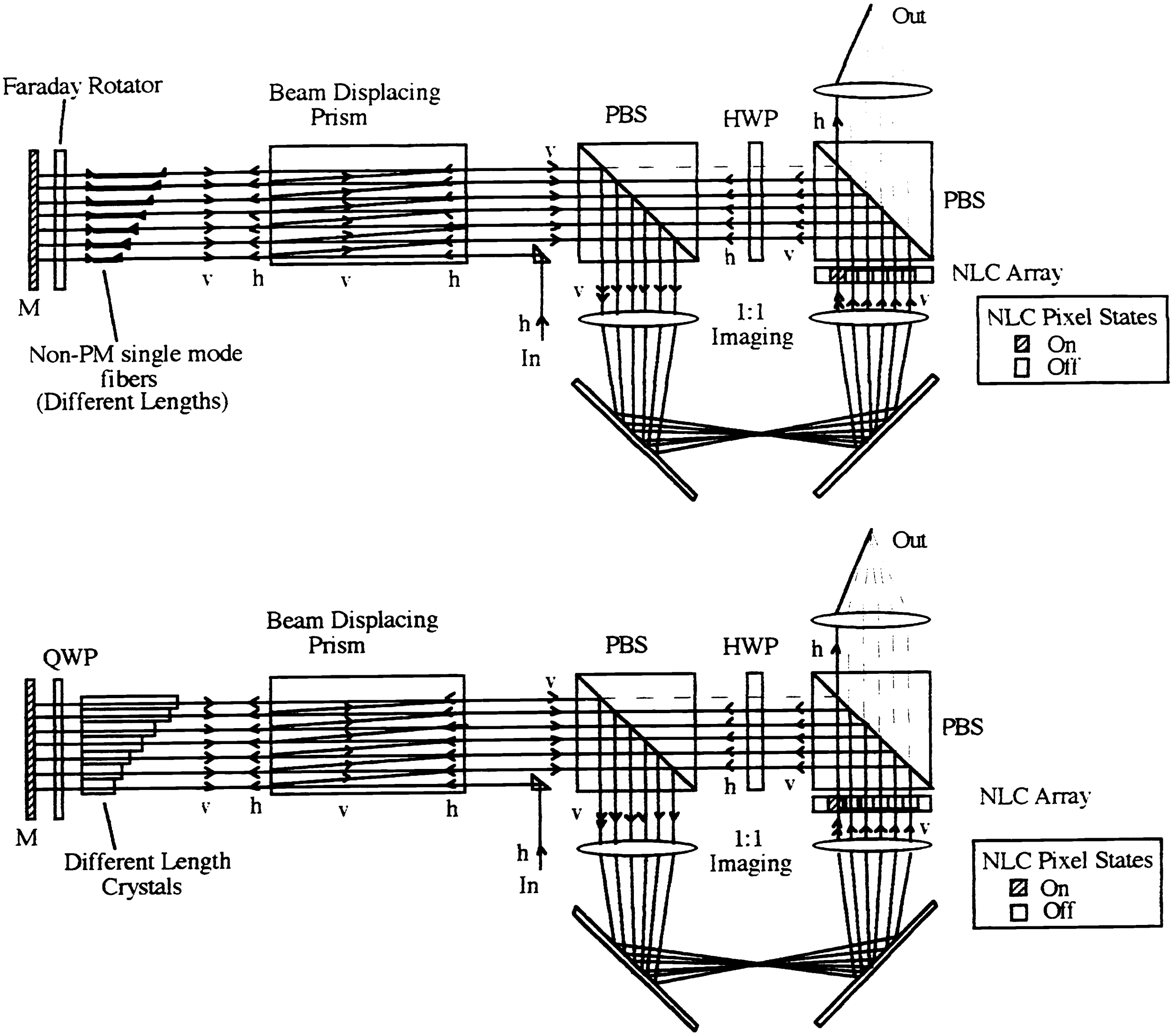

Fig.8 shows non-PM fiber and solid optics-based switched multichannel optical delay lines using beam displacing prisms.

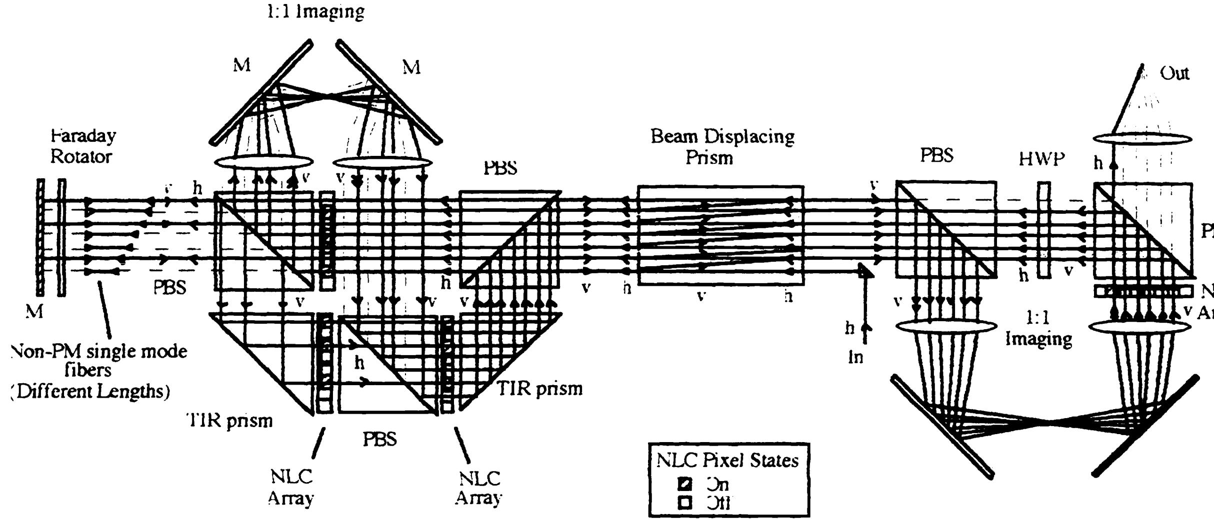

Fig.9 shows non-PM fiber-based switched multichannel binary M-bit fiber-optic delay line structure using beam displacing prisms.

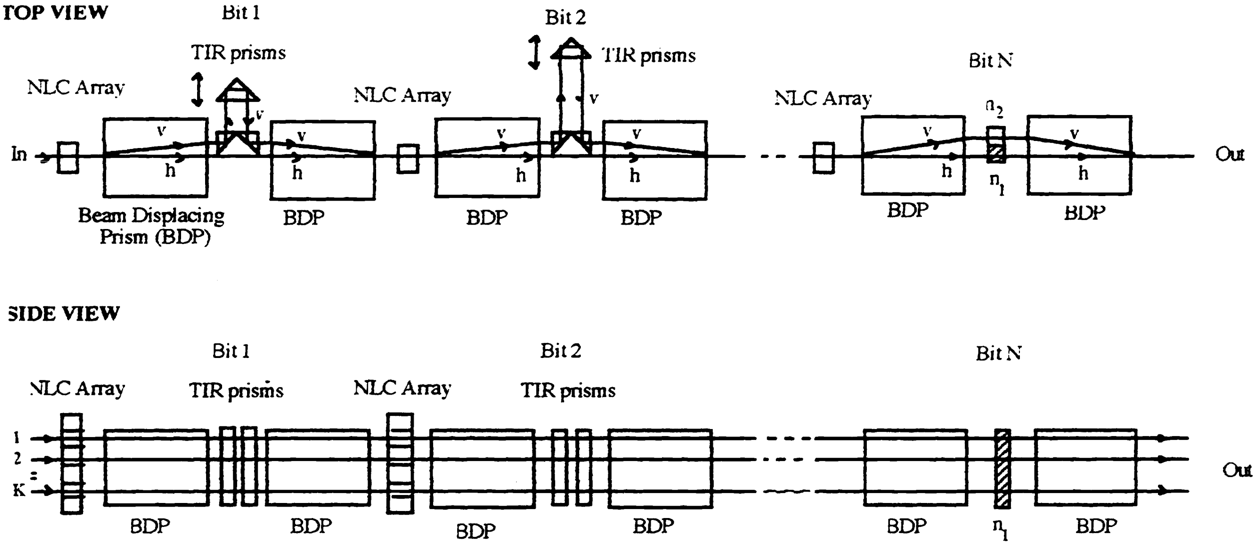

Fig.10 shows free-space/solid optics-based switched multichannel N-bit K-channel optical delay architecture using beam displacing prisms.